

The nature of aspidin and the evolutionary origin of bone

Joseph N. Keating^{1,2*}, Chloe L. Marquart¹, Federica Marone³ and Philip C. J. Donoghue^{1*}

Bone is the key innovation underpinning the evolution of the vertebrate skeleton, yet its origin is mired by debate over interpretation of the most primitive bone-like tissue, aspidin. This has variously been interpreted as cellular bone, acellular bone, dentine or an intermediate of dentine and bone. The crux of the controversy is the nature of unmineralized spaces pervading the aspidin matrix, which have alternatively been interpreted as having housed cells, cell processes or Sharpey's fibres. Discriminating between these hypotheses has been hindered by the limits of traditional histological methods. Here, we use synchrotron X-ray tomographic microscopy to reveal the nature of aspidin. We show that the spaces exhibit a linear morphology incompatible with interpretations that they represent voids left by cells or cell processes. Instead, these spaces represent intrinsic collagen fibre bundles that form a scaffold about which mineral was deposited. Aspidin is thus acellular dermal bone. We reject hypotheses that it is a type of dentine, cellular bone or transitional tissue. Our study suggests that the full repertoire of skeletal tissue types was established before the divergence of the earliest known skeletonizing vertebrates, indicating that the corresponding cell types evolved rapidly following the divergence of cyclostomes and gnathostomes.

The origin of the vertebrate mineralized skeleton, and of its canonical suite of cell and tissue types, predates the radiation of crown gnathostomes. Fossil jawless vertebrates, assigned to the gnathostome stem, therefore provide a unique record of the evolutionary assembly of the vertebrate skeleton¹. The Silurian–Devonian Heterostraci are of particular importance in this context, as they are considered among the most primitive skeletonizing vertebrates (Fig. 1). Consequently, heterostracan skeletal biology is integral to elucidating the nature of the primitive vertebrate skeleton. Skeletal tissues of early vertebrates, including heterostracans, are preserved routinely in astonishing detail², revealing cellular structure beyond the resolution of the most celebrated instances of exceptional preservation. Yet, in spite of this, the evolutionary significance of these ancient skeletons is obscured by controversy over the nature of the earliest bone-like tissue, aspidin. This controversy has, in turn, spilled into wider debate concerning the origin of the canonical repertoire of skeletal tissues. It has been argued that aspidin evidences an interval of plasticity between skeletal tissues before the evolutionary differentiation of skeletal cell types^{3,4}. To deduce the ancestral aspidin architecture, we studied taxa encompassing the breadth of heterostracan diversity. Hypotheses concerning the nature of aspidin hinge entirely on interpretation of unmineralized spaces, which pervade the aspidin biomineral matrix (Figs. 2 and 3). Correct interpretation of these structures requires characterization of their three-dimensional morphology and geometry within the aspidin matrix. Unfortunately, due to limitations inherent in two-dimensional invasive histological methods, the spaces have been poorly characterized. For example, some researchers have distinguished coarse ‘spindle-shaped’ spaces from fine-calibre ‘tubules’^{4–7}, while others have made no distinction between spaces^{8–11}. We used synchrotron X-ray tomographic microscopy (srXTM)^{12–17}, in addition to conventional invasive techniques, to characterize the histology of aspidin, as well as the three-dimensional morphology and architecture of the spaces pervading the tissue. These data permit direct histological comparison with the canonical skeletal tissues

of living vertebrates, allowing us to test hypotheses concerning the identity of the aspidin spaces and, in turn, reveal the nature of this enigmatic tissue.

Results

The heterostracan cephalothoracic skeleton (Fig. 2a) is four-layered (Fig. 2b,c), consisting of a superficial layer of dentine tubercles capped with enameloid, a compact reticular layer of canals (L1), a trabecular middle layer (L2) and a basal plywood-like layer of isopeidin (L3), sometimes referred to as ‘lamellar aspidin’. It is important to note that the term ‘aspidin’ was initially conceived to describe only the middle layer of the heterostracan dermal skeleton¹⁰. However, its use has subsequently been expanded to describe seemingly acellular dermal skeletal tissues in galeaspid, thelodonts and anaspids, despite the fact that these tissues differ from aspidin *sensu stricto* both in terms of topology and histology^{8,11,18,19}. We restrict the term aspidin to its original meaning, referring to the middle layer (L2) of the heterostracan cephalothoracic skeleton¹⁰. Aspidin developed around an extensive vascular network of anastomosing canals and/or interconnected polygonal cancellae (Fig. 2b,c). The cancellar trabecular walls are bipartite in construction (Fig. 3a,g,k), consisting of lamellar layers (next to the vascular lumina) and a homogenous biomineral core. The lamellar tissue developed centripetally, resulting in constriction of the vascular spaces¹¹. The mineral matrix consists of elongate bundles (reflecting the fabric of the original collagen mesh) measuring 1–3 µm in diameter, which form a circumferential interlaced fabric enveloping the vascular spaces (Figs. 3d,i and 4d).

Aspidin trabeculae are pervaded by unmineralized thread-like spaces, measuring approximately 2–5 µm in diameter and anywhere between 50 and >150 µm in length (Figs. 2d, 3a–k and 4a–c). These are preserved either as voids or diagenetic mineral infill. The spaces are linear; they do not bifurcate and show no ramifying processes (Fig. 4a). Within the trabecular walls, the spaces are oriented orthogonally to, and cross cut, the lamellar boundaries

¹School of Earth Sciences, University of Bristol, Bristol, UK. ²School of Earth and Environmental Sciences, University of Manchester, Manchester, UK.

³Swiss Light Source, Paul Scherrer Institut, Villigen, Switzerland. *e-mail: joseph.keating@manchester.ac.uk; phil.donoghue@bristol.ac.uk

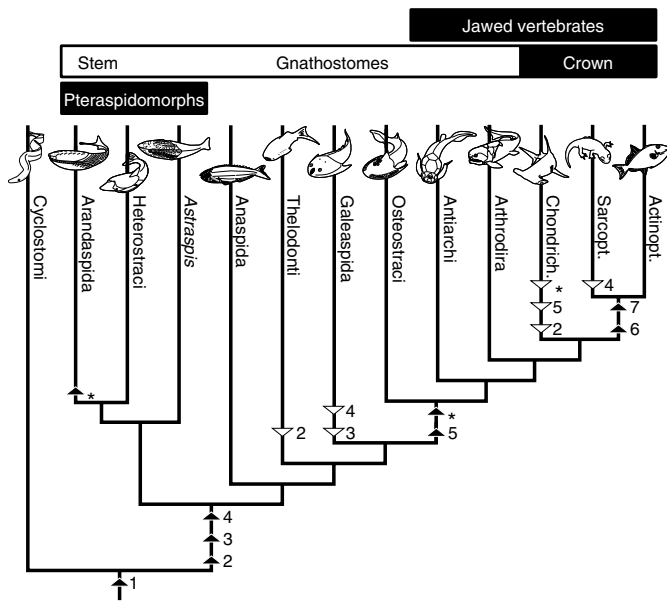


Fig. 1 | Hypothesis of vertebrate relations based on Keating and Donoghue¹⁷. Heterostracans, together with the Ordovician aged arandaspids and *Astraspis*, comprise the clade Pteraspidomorpha, interpreted as the sister group to all other ostracoderms and crown gnathostomes (that is, all other skeletonizing vertebrates). Based on our histological analyses, we inferred character evolution using parsimony under accelerated transformation (ACCTRAN) optimization. Black triangles represent character gain and white triangles represent character loss. Numbers represent cartilage (1), dermal bone (2), dentine (3), enamelioid (4), perichondral bone (5), endochondral bone (6) and enamel (7). Asterisks represent cell spaces in dermal bone.

(Figs. 2d, 3 and 4). Vertically, they are regularly spaced and approximately parallel to each other. The spaces are more numerous and densely packed at the base of the vasculature, close to the boundary with the basal plywood layer (Fig. 2b). At intersections between trabecular walls, the linear spaces transect one another at 55–90°, forming an interwoven lattice (Figs. 2d, 3e and 4c–e). Similarly, in taxa with thick trabecular walls, such as *Tesseraspis*, the thread-like spaces pervading the homogenous core of the trabeculae are aligned parallel to the lamellar outer layers, transecting orthogonally aligned spaces (Fig. 4e).

Discussion

The aspidin spaces are incompatible with the interpretation that they represent cell spaces^{4,5,20–22} because they are strictly linear without ramifying processes—a key characteristic of osteocyte lacunae. They are not ‘spindle shaped’ as has previously been suggested^{4,5,20,21}, but instead comprise elongate threads with a consistent diameter over the course of their length. The perceived spindle shape is an artefact of observing obliquely sectioned individual spaces, or else multiple overlapping spaces. They are also incompatible with osteocyte canaliculi, which are an order of magnitude smaller than the threads pervading the aspidin biomineral²³. They are of comparable size to dentine tubules, yet dentine is topologically incompatible with aspidin. Dentine is primarily a superficial dermal skeletal tissue, although it is occasionally deployed as a secondary mineralization tissue⁵, while aspidin makes up the primary tissue of the middle layer of the heterostracan skeleton. Morphological comparison between ‘true’ dentinal tubules, found in the tubercles decorating the surface of heterostracan dermal armour, and the aspidin spaces shows they differ markedly.

Of the competing interpretations of the aspidin spaces, only collagen is morphologically compatible. These spaces are far too coarse

to have housed individual fibres, yet they are of comparable size to collagen fibre bundles in mineralized tissues of living vertebrates²⁴. Two types of fibre bundle are found in the dermal skeleton, termed extrinsic (that is, Sharpey’s fibres) and intrinsic. Extrinsic fibre bundles function as attachment structures anchoring the dermal skeleton to the periosteum²⁵. As such, they tend to be concentrated at the margins of mineralized elements and rarely penetrate deeper into the skeleton. Indeed, extrinsic fibre bundles are associated with the basal plywood layer of the heterostracan dermal skeleton and are typically coarser, longer and less densely packed than aspidin fibre bundle spaces (Fig. 2b). In contrast, intrinsic collagen fibres are ubiquitous throughout dermal bone. In teleost acellular bone, intrinsic collagen fibres form bundles cross-cutting the contiguous lamellae of the mineralized matrix, in much the same manner as the aspidin spaces. These are unmineralized in life, and so form voids in the mineral matrix postmortem²⁶. The aspidin spaces are organized radially about cancellae and orthogonal to the circumferential mineralized collagen bundles (Figs. 2d and 4a–c), or else tangled at the boundaries between cancellae. They do not extend through the basal layer or superficial layer and, thus, could not have been used as attachment fibres to anchor the skeleton within the dermis. However, their organization is entirely compatible with intrinsic collagen. Cells migrating through a collagen mesh have been shown to organize fibres in two axes parallel and orthogonal to their migrating trajectory^{27,28}. Tensile forces induced by migrating fibroblasts organize collagen into ‘straps’ parallel to the course of cell migration²⁷. However, due to the nonlinear properties of collagen meshes, fibres are reorganized perpendicular to the migration direction in a process known as orthogonal amplification of mesh distortion²⁸. Thus, the aspidin structure suggests that, before mineralization, the collagen mesh is reorganized via cell migration, resulting in a circumferential fabric of straps parallel to fibroblast migration, as well as an orthogonal fabric of straps propagated by mesh distortion. The orthogonal straps together form an intrinsic scaffold of unmineralized collagen, about which mineralization of the mesh occurs.

Identification of aspidin spaces as voids housing unmineralized collagen permits reconsideration of aspidin homology and its significance in understanding the origin and early evolution of the vertebrate mineralized skeleton. Hypotheses that aspidin represents a type of dentine⁸ or intermediate between dentine and bone⁶ are based entirely on interpretation of the aspidin spaces as canaliculi, comparable to dentine tubules, which we have falsified. Rather, the histology of aspidin is entirely compatible with bone. Specifically, aspidin is topologically compatible with trabecular bone; that is, diploë comprising the intermediate layer of the dermatocranium of crown gnathostomes. In contrast with previous studies^{4,5,20–22}, we show that aspidin is acellular, in the sense that it contains no cell lacunae. There has been much debate over the primacy of cellular versus acellular bone, largely stemming from the fact that both bone types appear simultaneously in the fossil record³. However, ancestral state reconstruction allows us to resolve this controversy, revealing acellularity as the plesiomorphic condition, with cellular bone evolving from an acellular bone independently on at least two occasions: in the lineage leading to osteostracans and jawed vertebrates, and within pteraspidomorphs²⁹ (Fig. 1).

Identification of aspidin as acellular bone eliminates the last piece of evidence that early vertebrates exhibited a high degree of skeletal plasticity before differentiation of the canonical suite of skeletal tissues. Instead, our results, together with previous research^{2,7–11,30}, suggest that acellular bone, dentine and enamelioid were already established before the divergence of the known skeletonizing vertebrate clades. These tissue types appear simultaneously in the fossil record, and in topological co-ordination, without any precursor. One possible explanation for this punctuated appearance is that it records the evolutionary innovation of biomineralization.

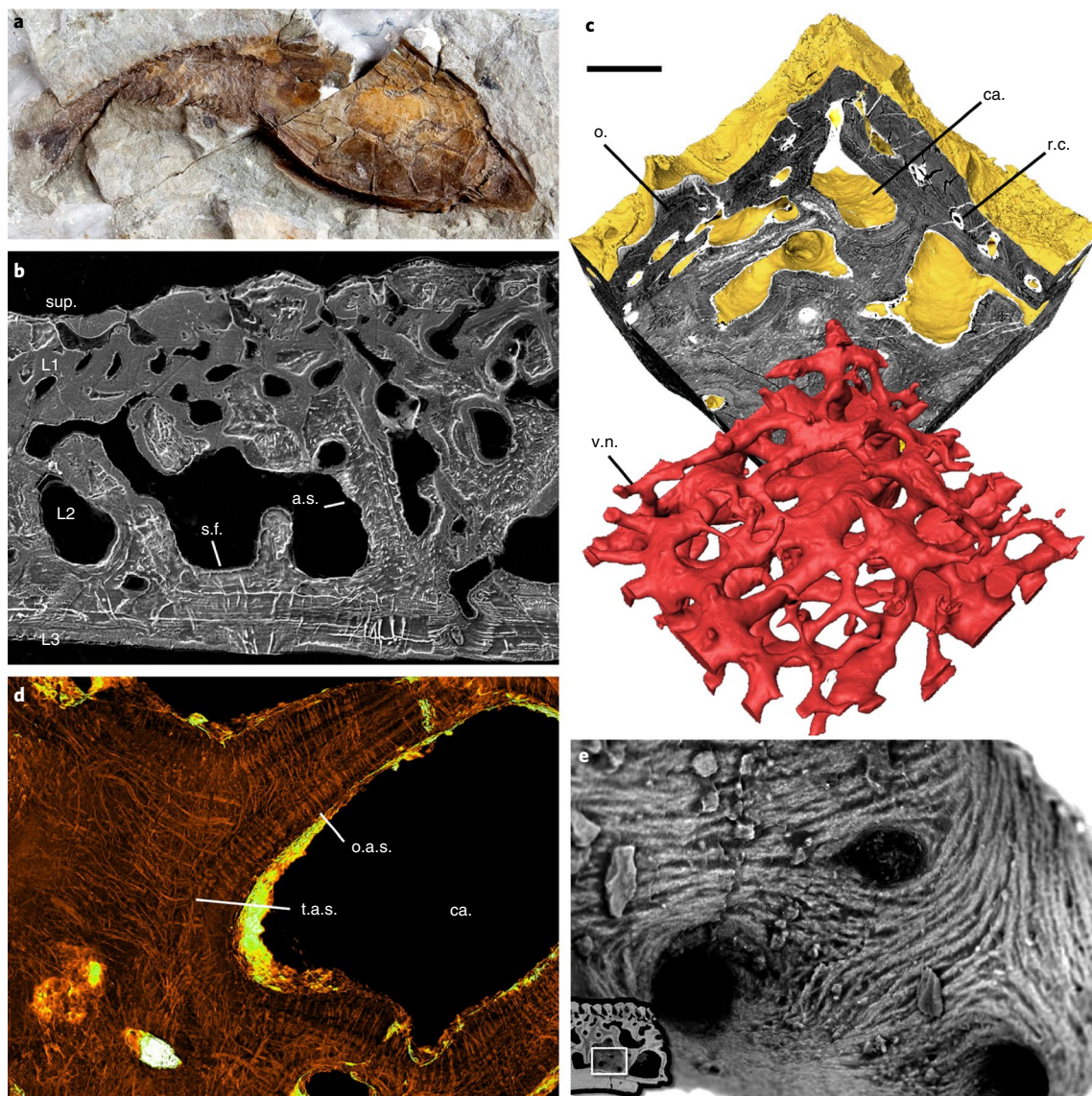


Fig. 2 | Morphology and histology of the heterostracan dermal skeleton. **a**, Gross external morphology of the dermal skeleton of *Errivaspis waynensis* (Natural History Museum, London (NHMUK) P19789) from the Lochkovian of Herefordshire, UK. **b**, Etched SEM section of *L. dairydinglensis* (NHMUK P75400) showing the four-layered construction of the dermal skeleton. Aspidin spaces and Sharpey's fibre spaces are preserved as high-relief pyrite diagenetic infill. Sharpey's fibre spaces pervading L3 can be distinguished from aspidin spaces in L2 by both their size and configuration. **c**, Sectioned srXTM virtual model of the dermal skeleton of *T. tessellata* (NHMUK P73617). The vasculature network is shown to comprise a series of cancellae interlinked by reticular canals. **d**, SrXTM horizontal virtual thin section through aspidin trabeculae of *T. tessellata* (NHMUK P73618). Aspidin spaces are preserved as diagenetic pyrite infill with high X-ray attenuation. Spaces are organized orthogonal to the trabecular lamellae, or else tangled at trabecular intersections. **e**, SEM detail of a cancellar chamber of *L. dairydinglensis* (NHMUK P73622), showing a centripetal fabric of coarse spicules, interpreted as mineralized (crystal) fibre bundles. a.s., aspidin space; ca., cancellae; L1, layer 1; L2, layer 2; L3, layer 3; o., odontode; o.a.s., orthogonal aspidin space; r.c., reticular canal; s.f., Sharpey's fibre space; sup., superficial layer; t.a.s., tangled aspidin space; v.n., vascular network. Relative scale bar: 21 mm in **a**, 183 μm in **b**, 165 μm in **c**, 83 μm in **d** and 49 μm in **e**.

It has been suggested that many of the key genes responsible for the synthesis of collagenous tissues emerged through duplication associated with whole-genome duplication (WGD) events early in vertebrate evolution, and redundant copies were subsequently co-opted for biomineralization^{31,32}. The origin of biomineralization has also been linked to the evolution of secretory calcium-binding phosphoprotein genes via tandem duplication following WGD. Unfortunately, the relative and absolute timing of early vertebrate WGD is poorly understood. Conventionally, two rounds of WGD are inferred to have occurred, either before³³ or either side of³⁴ the divergence of cyclostomes and gnathostomes. More recent analysis of the lamprey germline genome casts doubt on these scenarios,

preferring instead a single WGD preceded by a series of large segmental duplications^{35,36}. Additional insight from hagfish and elasmobranch genomes will help resolve the tempo of vertebrate genomic evolution and provide a test for hypotheses concerning the punctuated appearance of mineralized tissues in the fossil record.

The nature of aspidin has proved elusive since it was first described over 80 years ago. We show that the unmineralized aspidin spaces, which have provoked such controversy, are best interpreted as a scaffold of collagen fibre bundles, about which mineral was deposited. These spaces are aligned orthogonal to a radial fabric of mineralized fibre bundles, which circumscribe the polygonal cancellae. The organization of these fabrics is consistent

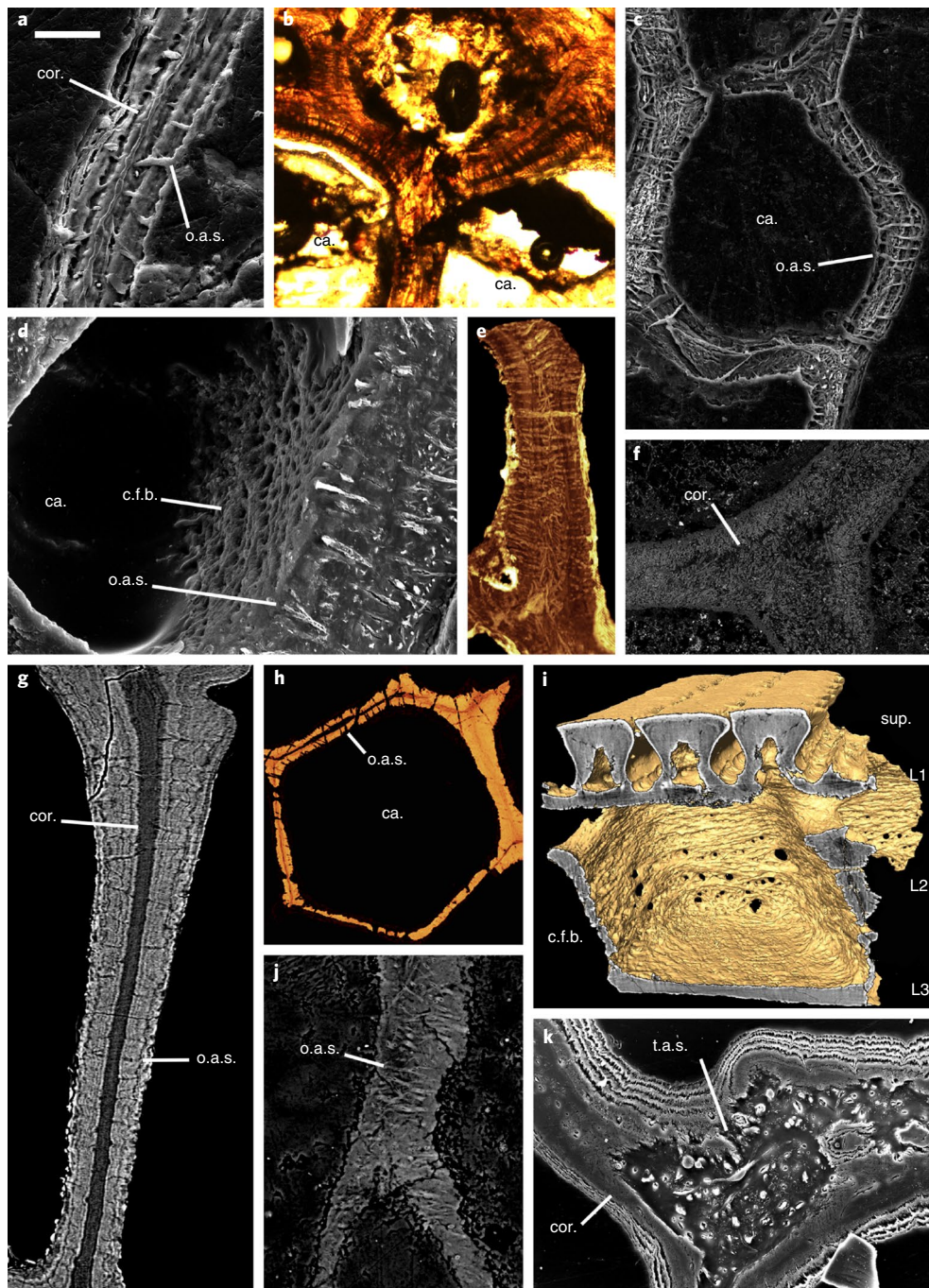


Fig. 3 | Histology of aspidin in phylogenetically disparate heterostracan taxa. **a**, SEM etched section of a trabecular wall of *L. serrata* Swedish Museum of Natural History (NRM-PAL) C.5940 showing bipartite construction. **b**, Light microscopy thin section of a junction of trabecular walls of *P. symondsii* NHMUK P73619. **c**, Etched SEM section through a polygonal cancellar chamber of *C. kingi* NHMUK P73616. **d**, Backscatter detector scanning electron microscopy (BSD SEM) vertical section through a polygonal cancellar chamber of *C. kingi* NHMUK P73613, showing both the aspidin spaces and crystal fibre bundles. **e**, Horizontal SrXTM virtual thin section through trabecular walls of *T. tessellata* NHMUK P73617. **f**, BSD SEM section of a trabecular junction of *Amphiaspis* species GIT 313-32. **g**, SrXTM tomographic slice through a vertical trabecular of *A. macculloughi* NHMUK P73620. **h**, SrXTM horizontal virtual thin section through a polygonal cancellar chamber of *Pteraspis* species NRM-PAL C.5945. **i**, Isosurface model of the same specimen showing the circular fabric of fibres enveloping the cancellae. **j**, Vertical trabecular wall of *Poraspis* species NHMUK P17957. **k**, Junction of trabecular walls of *L. dairyinglensis* NHMUK P73623. ca., cancellae; c.f.b., crystal fibre bundles; cor., homogenous core of bipartite aspidin trabeculae; L1, layer 1; L2, layer 2; L3, layer 3; o.a.s., orthogonal aspidin space; sup., superficial layer; t.a.s., tangled aspidin space. Relative scale bar: 30 μm in **a**, 48 μm in **b**, 79 μm in **c**, 30 μm in **d**, 88 μm in **e**, 180 μm in **f**, 41 μm in **g**, 100 μm in **h**, 91 μm in **i**, 40 μm in **j** and 52 μm in **k**.

with orthogonal amplification of mesh distortion via osteoblast migration. These data identify aspidin as acellular dermal bone. Hypotheses that it comprises a cellular type of bone, a type of dentine or an intermediate tissue grade are rejected. Our study

suggests that the full repertoire of skeletal cell and tissue types was already established in the earliest known skeletonizing vertebrates (Fig. 1)—a consequence of expansion of neural crest cell fates following the divergence of cyclostomes and gnathostomes³⁷.

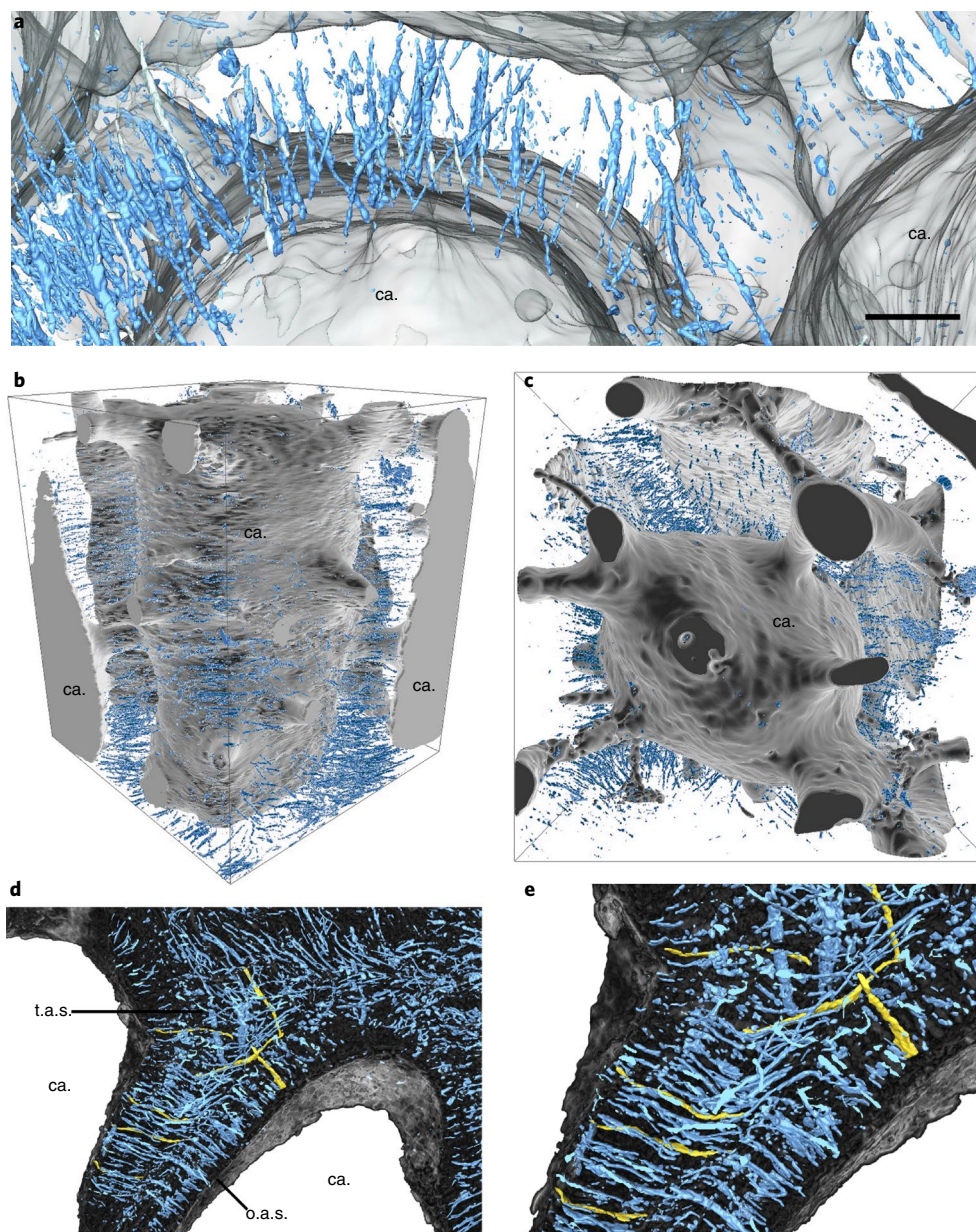


Fig. 4 | SrXTM virtual segmentation of aspidin spaces in *L. dairydinglensis* and *T. tessellata*. **a**, Detail of orthogonal aspidin spaces pervading the trabecular walls dividing polygonal cancellae in *L. dairydinglensis* (NHMUK P75401). These spaces exhibit linear morphology without ramifications, precluding interpretation that these are cell or cell process spaces. **b,c**, Lateral (**b**) and transverse (**c**) views of the organization of aspidin spaces in *L. dairydinglensis* (NHMUK P75401) radiating about a polygonal cancellar vacuity. **d**, Horizontal section of the middle layer of *T. tessellata* (NHMUK P73617) showing orthogonal aspidin spaces within the trabeculae and tangled aspidin spaces at the intersection between trabeculae. Several orthogonal and tangled spaces have been segmented individually (highlighted in gold) to illustrate their linear, non-branching morphology. **e**, Magnified image from **d**. *ca.*, cancellae; *o.a.s.*, orthogonal aspidin space; *t.a.s.*, tangled aspidin space. Relative scale bar: 55 μm in **a**, 189 μm in **b**, 160 μm in **c**, 92 μm in **d** and 50 μm in **e**.

Methods

The material of this study originates from a number of geological localities. *Lepidaspis serrata* and *Pteraspis* species material is from the Drake Bay Formation of Prince of Wales Island in the Canadian Arctic Archipelago, and is stored at the Naturhistoriska Riksmuseet, Stockholm (NRM). The *Tesseraspis tessellata*, *Phialaspis symondsii*, *Corvaspis kingi* and *Anglaspis macculoughi* material is from a small stream section at Earnstrey Hall Farm, Shropshire, UK, and is stored at the Natural History Museum, London (NHM). *Loricopteraspis dairydinglensis* is from a stream section in nearby Dairy Dingle, and is also stored at the NHM and at the University of Bristol. *Rhinopteraspis crouchi* material is from Cradley, Herefordshire, and is stored at the NHM. The *Poraspis* species material comes from Jagilnytsia Stara, Podolia, Ukraine, and is stored at the NHM. The *Psammosteus megalopteryx* specimen was received from the collection of the late B. Halstead and is of unknown provenance. It has been accessioned at the NHM.

Scanning electron microscopy (SEM). Specimens were embedded using EpoFix resin (Struers) and left to cure for at least 24 h. Sections were cut using an IsoMet low speed saw (Buehler). Cut surfaces were impregnated using EPO-THIN Resin (Buehler). Small specimens were then mounted in 25-mm-diameter aluminium rings using EpoFix (Buehler). All specimens were ground manually using P800 to P4000 grit paper. IsoCut Fluid (Buehler) was used for lubrication during grinding. Large sections were polished manually using MetaDi 3 and 1 μm Diamond Paste (Buehler). Following 24 h of curing, specimens were ground manually using P1200 to P4000 grit paper. Specimens mounted in aluminium rings were polished using an EcoMet 250 Grinder/Polisher (Buehler) with MetaDi 3 and 1 μm suspensions. Selected polished sections were etched using 5% orthophosphoric acid (H_3PO_4) for 1–2 min. Polished specimens were carbon coated using the K450 carbon coater (Emitech). Images were taken using a Hitachi S-3500N scanning electron microscope. SEM analysis was conducted at the University of Bristol School of Earth Science's Electron Microbeam Facility.

Light microscopy. Light microscopy thin sections were examined using a Leica M205C microscope with a 2× Plan Achromat lens, and imaged with a Leica DFC425C digital camera. Sections were analysed using both bright-field and Nomarski differential interference contrast microscopy.

Synchrotron radiation X-ray tomographic microscopy. SrXTM experiments were conducted at the X04SA-MS and X02DA-TOMCAT beamlines of the Swiss Light Source, Paul-Scherrer Institut, Villigen, Switzerland. Measurements were taken using 10× and 20× objective lenses, 13–25 keV, and 180–2,500 ms exposure times. For each dataset, 1,501 equiangular projections were acquired over 180°. These were post-processed and rearranged into flat- and dark-field-corrected sinograms. Reconstruction was performed on a Linux PC cluster using a highly optimized routine based on the Fourier transform method and a regridding procedure, resulting in volumetric data with voxel dimensions of 0.65 μm (10× objective) and 0.325 μm (20× objective). The data were analysed using Avizo 8.0 (<https://www.fei.com/software/amira-avizo/>). Tomographic sections were produced using the orthoslice module. Virtual thin sections were produced using the volume rendering module. The data were cropped, producing thin sections 10–100 slices thick. Aspidin vasculature and spaces were modelled using the virtual segmentation module.

Reporting Summary. Further information on experimental design is available in the Nature Research Reporting Summary linked to this article.

Data availability. The specimens on which this study was based are deposited at the NHM (NHMUK), Swedish Museum of Natural History (NRM-PAL) and School of Earth Sciences, University of Bristol. The supporting tomographic datasets are available from the University of Bristol data repository (data.bris.ac.uk) at <https://data.bris.ac.uk/data/dataset/1agbdxus79jan27rsyl580oxp>.

Received: 30 November 2017; Accepted: 27 June 2018;

Published online: 31 July 2018

References

- Donoghue, P. C. J. & Keating, J. N. Early vertebrate evolution. *Palaeontology* **57**, 879–893 (2014).
- Donoghue, P. C. J. & Sansom, I. J. Origin and early evolution of vertebrate skeletonization. *Microsc. Res. Tech.* **59**, 352–372 (2002).
- Smith, M. M. & Hall, B. K. Development and evolutionary origins of vertebrate skeletogenic and odontogenic tissues. *Biol. Rev.* **65**, 277–373 (1990).
- Halstead, L. B. Calcified tissues in the earliest vertebrates. *Calcif. Tissue Int.* **3**, 107–124 (1969).
- Halstead Tarlo, L. B. Psammosteiformes (Agnatha) - A review with descriptions of new material from the Lower Devonian of Poland. I - General part. *Palaeontol. Polonica* **13**, 1–135 (1964).
- Halstead, L. B. The heterostracan fishes. *Biol. Rev.* **48**, 279–332 (1973).
- Ørving, T. Histologic studies of ostracoderms, placoderms and fossil elasmobranchs. 6. Hard tissues of Ordovician vertebrates. *Zool. Scr.* **18**, 427–446 (1989).
- Denison, R. H. Ordovician vertebrates from western United States. *Fieldiana Geol.* **16**, 131–192 (1967).
- Bystrow, A. P. The microstructure of skeleton elements in some vertebrates from Lower Devonian deposits of the USSR. *Acta Zool.* **40**, 59–83 (1959).
- Gross, W. Die fische des mittleren Old Red Südlivlands. *Palaeont. Abh.* **18**, 123–156 (1930).
- Gross, W. Histologische studien am aussenskelett fossiler agnathen und fische. *Palaeontogr. Abt. A* **83**, 1–60 (1935).
- Donoghue, P. C. J. et al. Synchrotron X-ray tomographic microscopy of fossil embryos. *Nature* **442**, 680–683 (2006).
- Tafforeau, P. et al. Applications of X-ray synchrotron microtomography for non-destructive 3D studies of paleontological specimens. *Appl. Phys. A* **83**, 195–202 (2006).
- Rucklin, M. et al. Development of teeth and jaws in the earliest jawed vertebrates. *Nature* **491**, 748–753 (2012).
- Sanchez, S., Ahlberg, P. E., Trinajstić, K. M., Mirone, A. & Tafforeau, P. Three-dimensional synchrotron virtual paleohistology: a new insight into the world of fossil bone microstructures. *Microsc. Microanal.* **18**, 1095–1105 (2012).
- Qu, Q., Blom, H., Sanchez, S. & Ahlberg, P. Three-dimensional virtual histology of Silurian osteostracan scales revealed by synchrotron radiation microtomography. *J. Morphol.* **276**, 873–888 (2015).
- Keating, J. N. & Donoghue, P. C. J. Histology and affinity of anaspids, and the early evolution of the vertebrate dermal skeleton. *Proc. R. Soc. B* **283**, 20152917 (2016).
- Märss, T. A new Late Silurian or Early Devonian thelodont from the Boothia Peninsula, Arctic Canada. *Palaeontology* **42**, 1079–1099 (1999).
- Zhu, M. & Janvier, P. The histological structure of the endoskeleton in galeaspids (Galeaspida, Vertebrata). *J. Vertebr. Paleontol.* **18**, 650–654 (1998).
- Rohon, J. V. Die obersilurischen Fische von Oesel. II Theil. Selachii, Dipnoi, Ganoidei, Pteraspidae und Cephalaspidae. *Mem. Acad. Sci. St Petersburg* **41**, 1–124 (1893).
- Halstead Tarlo, L. B. Aspidin: the precursor of bone. *Nature* **199**, 46–48 (1963).
- Novitskaya, L. I. in *Psammosteids (Agnatha, Psammosteidae) of the Devonian of the USSR* (eds Obruchev, D. & Mark-Kurik, E.) 257–282 (Geological Institute of the Estonian Academy of Sciences, 1966).
- You, L. D., Weinbaum, S., Cowin, S. C. & Schaffler, M. B. Ultrastructure of the osteocyte process and its pericellular matrix. *Anat. Rec. A* **278**, 505–513 (2004).
- Höhling, H., Kreilos, R., Neubauer, G. & Boyde, A. Electron microscopy and electron microscopical measurements of collagen mineralization in hard tissues. *Z. Zellforsch. Mikrosk. Anat.* **122**, 36–52 (1971).
- Aaron, J. E. Periosteal Sharpey's fibers: a novel bone matrix regulatory system. *Front. Endocrinol.* **3**, 1–10 (2012).
- Moss, M. L. The biology of acellular teleost fish bone. *Ann. NY Acad. Sci.* **109**, 337–350 (1963).
- Petroll, W. M., Cavanagh, H. D. & Jester, J. V. Dynamic three-dimensional visualization of collagen matrix remodeling and cytoskeletal organization in living corneal fibroblasts. *Scanning* **26**, 1–10 (2004).
- Sawhney, R. K. & Howard, J. Slow local movements of collagen fibers by fibroblasts drive the rapid global self-organization of collagen gels. *J. Cell Biol.* **157**, 1083–1092 (2002).
- Sansom, I. J., Haines, P. W., Andreev, P. & Nicoll, R. S. A new pteraspidomorph from the Nibel Formation (Katian, Late Ordovician) of the Canning Basin, Western Australia. *J. Vertebr. Paleontol.* **33**, 764–769 (2013).
- Keating, J. N., Marquart, C. L. & Donoghue, P. C. J. Histology of the heterostracan dermal skeleton: insight into the origin of the vertebrate mineralised skeleton. *J. Morphol.* **276**, 657–680 (2015).
- Kawasaki, K., Buchanan, A. V. & Weiss, K. M. Biomineralization in humans: making the hard choices in life. *Annu. Rev. Genet.* **43**, 119–142 (2009).
- Huxley-Jones, J., Robertson, D. L. & Boot-Handford, R. P. On the origins of the extracellular matrix in vertebrates. *Matrix Biol.* **26**, 2–11 (2007).
- Kuraku, S., Meyer, A. & Kuratani, S. Timing of genome duplications relative to the origin of the vertebrates: did cyclostomes diverge before or after? *Mol. Biol. Evol.* **26**, 47–59 (2009).
- Holland, P. W., Garcia-Fernández, J., Williams, N. A. & Sidow, A. Gene duplications and the origins of vertebrate development. *Development* **1994**, 125–133 (1994).
- Smith, J. J. & Keinath, M. C. The sea lamprey meiotic map improves resolution of ancient vertebrate genome duplications. *Genome Res.* **25**, 1081–1090 (2015).
- Smith, J. J. et al. The sea lamprey germline genome provides insights into programmed genome rearrangement and vertebrate evolution. *Nat. Genet.* **50**, 270–277 (2018).
- Donoghue, P. C. J., Graham, A. & Kelsh, R. N. The origin and evolution of the neural crest. *BioEssays* **30**, 530–541 (2008).

Acknowledgements

We thank J. Cunningham (University of Bristol), M. Rucklin (Naturalis, Leiden) and C. Martinez-Perez (University of Valencia) for beamline assistance, E. Bernard (NHM, London) for collections services, and S. Kearns (University of Bristol) for assistance at the Bristol Earth Sciences Microprobe Facility. We thank G. Koentges (University of Warwick) and I. Sansom (University of Birmingham) for discussion. J.N.K. was funded by a NERC Studentship. P.C.J.D. is funded by the NERC (NE/P013678/1, NE/N002067/1 and NE/G016623/1) and BBSRC (BB/N000919/1). C.L.M. completed this work in partial fulfilment of the MSc Palaeobiology at the University of Bristol.

Author contributions

J.N.K. and P.C.J.D. conceived the project. P.C.J.D. and C.L.M. prepared the histological sections. J.N.K., E.M. and P.C.J.D. collected the tomographic data. J.N.K. and C.L.M. processed the tomographic data. All authors contributed towards data interpretation and writing of the manuscript.

Competing interests

The authors declare no competing interests.

Additional information

Supplementary information is available for this paper at <https://doi.org/10.1038/s41559-018-0624-1>.

Reprints and permissions information is available at www.nature.com/reprints.

Correspondence and requests for materials should be addressed to J.N.K. or P.C.J.D.

Publisher's note: Springer Nature remains neutral with regard to jurisdictional claims in published maps and institutional affiliations.

Reporting Summary

Nature Research wishes to improve the reproducibility of the work that we publish. This form provides structure for consistency and transparency in reporting. For further information on Nature Research policies, see [Authors & Referees](#) and the [Editorial Policy Checklist](#).

Statistical parameters

When statistical analyses are reported, confirm that the following items are present in the relevant location (e.g. figure legend, table legend, main text, or Methods section).

n/a Confirmed

- The exact sample size (n) for each experimental group/condition, given as a discrete number and unit of measurement
- An indication of whether measurements were taken from distinct samples or whether the same sample was measured repeatedly
- The statistical test(s) used AND whether they are one- or two-sided
Only common tests should be described solely by name; describe more complex techniques in the Methods section.
- A description of all covariates tested
- A description of any assumptions or corrections, such as tests of normality and adjustment for multiple comparisons
- A full description of the statistics including central tendency (e.g. means) or other basic estimates (e.g. regression coefficient) AND variation (e.g. standard deviation) or associated estimates of uncertainty (e.g. confidence intervals)
- For null hypothesis testing, the test statistic (e.g. F , t , r) with confidence intervals, effect sizes, degrees of freedom and P value noted
Give P values as exact values whenever suitable.
- For Bayesian analysis, information on the choice of priors and Markov chain Monte Carlo settings
- For hierarchical and complex designs, identification of the appropriate level for tests and full reporting of outcomes
- Estimates of effect sizes (e.g. Cohen's d , Pearson's r), indicating how they were calculated
- Clearly defined error bars
State explicitly what error bars represent (e.g. SD, SE, CI)

Our web collection on [statistics for biologists](#) may be useful.

Software and code

Policy information about [availability of computer code](#)

Data collection

N/A

Data analysis

N/A

For manuscripts utilizing custom algorithms or software that are central to the research but not yet described in published literature, software must be made available to editors/reviewers upon request. We strongly encourage code deposition in a community repository (e.g. GitHub). See the Nature Research [guidelines for submitting code & software](#) for further information.

Data

Policy information about [availability of data](#)

All manuscripts must include a [data availability statement](#). This statement should provide the following information, where applicable:

- Accession codes, unique identifiers, or web links for publicly available datasets
- A list of figures that have associated raw data
- A description of any restrictions on data availability

Data availability. The specimens on which this study was based are deposited at the Natural History Museum, London (NHMUK), Swedish Museum of Natural History (NRM-PAL) and the University of Bristol, School of Earth Sciences (BRSUG). The supporting tomographic and phylogenetic datasets are available from the University of Bristol data repository (data.bris) at <https://doi.org/10.5523/bris.XXXX>.

Field-specific reporting

Please select the best fit for your research. If you are not sure, read the appropriate sections before making your selection.

Life sciences Behavioural & social sciences Ecological, evolutionary & environmental sciences

For a reference copy of the document with all sections, see [nature.com/authors/policies/ReportingSummary-flat.pdf](https://www.nature.com/authors/policies/ReportingSummary-flat.pdf)

Ecological, evolutionary & environmental sciences study design

All studies must disclose on these points even when the disclosure is negative.

Study description	We conducted Synchrotron Radiation X-ray Tomographic Microscopy experiments to investigate the dermal skeleton of the most primitive fossil vertebrates. Our study combines SrXTM results with histological data obtained using conventional destructive microscopy techniques (e.g. SEM, LM). We sampled taxa representative of the phylogenetic diversity of the heterostraci, an extinct group of jawless fishes. Our data reveal the nature of the poorly understood skeletal tissue known as 'aspidin', and elucidate the evolution of the vertebrate dermal skeleton.
Research sample	The material of this study originates from a number of geological localities. <i>Lepidaspis serrata</i> and <i>Pteraspis</i> sp. material is from the Drake Bay Formation of Prince of Wales Island in the Canadian Arctic Archipelago and is stored at the Naturhistoriska Riksmuseet, Stockholm (NRM). The <i>Tesseractaspis tessellata</i> , <i>Phialaspis symondsi</i> , <i>Corvaspis kingi</i> and <i>Anglaspis macculloughi</i> material is from a small stream section at Earnstrey Hall Farm, Shropshire, UK and is stored at the Natural History Museum, London (NHM). <i>Loricopteraspis dairyinglensis</i> is from a stream section in nearby Dairy Dingle and is also stored at the NHM and at the University of Bristol. <i>Rhinopteraspis crouchi</i> material is from Cradley, Herefordshire and is stored at the NHM. The <i>Poraspis</i> sp. material comes from Jagilnytsia Stara, Podolia, Ukraine, and is stored at the NHM. The <i>Psammosteus megalopteryx</i> specimen was received from the collection of the late Beverly Halstead and is of unknown provenance. It has been accessioned at the NHM.
Sampling strategy	We sampled fossil dermal skeletal fragments of a range of taxa representative of the phylogenetic diversity of the Heterostraci, an extinct group of jawless fishes.
Data collection	SrXTM data were collected at the Swiss Light Source at beamtime sessions in 2007 and 2012. Data were collected by P. Donoghue, J. Keating and C. Marquart. SEM and LM images were collected by J. Keating in 2012 and C. Marquart in 2007.
Timing and spatial scale	Our data are not time series.
Data exclusions	No data were excluded from our study.
Reproducibility	We have included the models and raw slice data of our tomographic analyses. Thus the models that we have produced are both reproducible and verifiable. All material used in the study has been accessioned in international collections and consequently the observations from LM and SEM analysis are also reproducible and verifiable.
Randomization	This is not relevant to our study because we are dealing with small numbers of available specimens.
Blinding	Blinding was not relevant to our study. There is no bias for which we can be blinded that can alter the results of our synchrotron experiments.
Did the study involve field work?	<input type="checkbox"/> Yes <input checked="" type="checkbox"/> No

Reporting for specific materials, systems and methods

Materials & experimental systems

- | | |
|-------------------------------------|--|
| n/a | Included in the study |
| <input checked="" type="checkbox"/> | <input type="checkbox"/> Unique biological materials |
| <input checked="" type="checkbox"/> | <input type="checkbox"/> Antibodies |
| <input checked="" type="checkbox"/> | <input type="checkbox"/> Eukaryotic cell lines |
| <input type="checkbox"/> | <input checked="" type="checkbox"/> Palaeontology |
| <input checked="" type="checkbox"/> | <input type="checkbox"/> Animals and other organisms |
| <input checked="" type="checkbox"/> | <input type="checkbox"/> Human research participants |

Methods

- | | |
|-------------------------------------|---|
| n/a | Included in the study |
| <input checked="" type="checkbox"/> | <input type="checkbox"/> ChIP-seq |
| <input checked="" type="checkbox"/> | <input type="checkbox"/> Flow cytometry |
| <input checked="" type="checkbox"/> | <input type="checkbox"/> MRI-based neuroimaging |

Palaeontology

Specimen provenance

The material of this study originates from a number of geological localities. *Lepidaspis serrata* and *Pteraspis* sp. material is from the Drake Bay Formation of Prince of Wales Island in the Canadian Arctic Archipelago and is stored at the Naturhistoriska Riksmuseet, Stockholm (NRM). The *Tesseractaspis tessellata*, *Phialaspis symondsi*, *Corvaspis kingi* and *Anglaspis macculloughi* material is from a small stream section at Earnstrey Hall Farm, Shropshire, UK and is stored at the Natural History Museum, London (NHM). *Loricopteraspis dairydinglensis* is from a stream section in nearby Dairy Dingle and is also stored at the NHM and at the University of Bristol. *Rhinopteraspis crouchi* material is from Cradley, Herefordshire and is stored at the NHM. The *Poraspis* sp. material comes from Jagilnytsia Stara, Podolia, Ukraine, and is stored at the NHM. The *Psammosteus megalopteryx* specimen was received from the collection of the late Beverly Halstead and is of unknown provenance. It has been accessioned at the NHM.

Specimen deposition

he specimens on which this study was based are repositated at the Natural History Museum, London (NHMUK), Swedish Museum of Natural History (NRM-PAL) and the University of Bristol, School of Earth Sciences (BRSUG).

Dating methods

No new dates are provided

Tick this box to confirm that the raw and calibrated dates are available in the paper or in Supplementary Information.